

Electrosynthesis and Characterization of a Novel Electrochromic Copolymer Based on 1,4-bis(2-(3,4-ethylenedioxy)thienyl)benzene and 1,4-bis(3-methylthiophen-2-yl)benzene

Wei Yang^{1,2}, Jinsheng Zhao^{1,3*}, Ying Kong^{2,3*}, Chuansheng Cui¹, Peng Li²

¹ Shandong Provincial Key laboratory of Chemical Energy Storage and Novel Cell Technology, Liaocheng University, Liaocheng, 252059, P. R. China

² State Key Laboratory of Heavy Oil Processing, China University of Petroleum (East China), Qingdao, 266555, P. R. China

³ State Key Laboratory of Electronic Thin Films and Integrated Devices, University of electronic Science and Technology of China, Chengdu, 610054, P. R. China

*E-mail: yingkong1967@yahoo.com.cn (Y. Kong); j.s.zhao@163.com (J.S.Zhao)

Received: 9 October 2012 / Accepted: 28 October 2012 / Published: 1 December 2012

In this article, successfully electrochemical copolymerization of the 1,4-bis(3-methylthiophen-2-yl)benzene (BMTB) monomer and the 1,4-bis(2-(3,4-ethylenedioxy)thienyl)benzene (EBE) monomer is used to fulfill a strategy in achieving desired fine tuning band gap copolymer. Cyclic voltammetry (CV), UV-vis, FT-IR and SEM analyses characterized the copolymer. Moreover, the copolymer film P(EBE-co-BMTB) displayed distinct color change between orange yellow, yellowish green, sky blue and purplish blue, and revealed different electrochromic properties from that of the PEBE and PBMTB film. Maximum contrast ($\Delta T\%$) of the P(EBE-co-BMTB) film is 31.1% and the response time of the film is 0.41 s from the oxidized to the reduced state at 430 nm. The P(EBE-co-BMTB) film showed satisfactory electrochromic properties and optical contrast. Electrochromic device (ECD) based on P(EBE-co-BMTB) and poly(3,4-ethylenedioxythiophene) (PEDOT) is also constructed and characterized. This ECD showed a maximum optical contrast ($\Delta T\%$) of 24.5% with a coloration efficiency (CE) of 397.9 cm² C⁻¹ at 630 nm. The neutral state of device shows grayish green color, while oxidized state reveals sky blue color.

Keywords: Electrochemical polymerization; Conjugated polymers; Electrochromism; 1,4-Bis(2-(3,4-ethylenedioxy)thienyl)benzene; 1,4-Bis(3-methylthiophen-2-yl)benzene

1. INTRODUCTION

The electrochromic materials based on conjugated polymers have become one of the main research topics due to their notable advantages. The conjugated polymers have low processing cost, high coloration efficiency, fast switching ability and fine-tuning of the band gap (and the color) [1]. They have been widely applied in organic light emitting diodes (OLEDs), organic field-effect transistors (OFETs), electrochromism and organic solar cells (OSCs) [2–5]. For conjugated polymers, the electrochromism is related to changing of band gaps during the doping-dedoping process, the doping process modifies the polymer electronic structure, producing new electronic states in the band gap, causing color changes [6]. Thus, the electrochromic properties of conducting polymers could be varied over a wide range by controlling the band gap of the polymer via proper choice of heteroaromatic ring and substituents [7, 8]. Although there are some reports on multichromic materials [9,10], it is still important to achieve materials that display distinctive colors upon applied potential. Hence, a major focus in the study of electrochromic polymer materials has been that of controlling their colors by main-chain and pendant group structural modification as well as copolymerization. Copolymerization is an easy, facile method to combine the electrochromic properties of the monomers [11]. The copolymerization of distinct monomers or homopolymerization of blending monomers containing several distinct units can lead to an appealing combination of the properties of the parent polymers [12].

Among electrochromic conjugated materials, thiophenes are a class of important polymers because of their high electrical conductivity, good redox property and facile band gap (E_g) tunability through structural modification [13–15]. In recent years, polymers containing alternating bithiophene and phenylene repeat units have been roused a great deal of interest, and some polymers with such structure have been synthesized and characterized [16–18]. Our group had synthesized the monomer of 1,4-bis(3-methylthiophen-2-yl)benzene (BMTB), based on which the PBMTB polymer was electrochemically synthesized, and the electrochromic properties of the polymer was studied in detail [19]. Besides, the monomer of 1,4-bis(2-(3,4-ethylenedioxy)thienyl)benzene (EBE) and its polymer PEBE have also been synthesized, and their band gap values (E_g) are somewhat lower than that of BMTB and PBMTB, respectively [10,20]. It is anticipated that the introduction of the EBE units into the PBMTB chains might be able to fine tune the band gap of the resultant copolymer, and then to modify the electrochromic properties of the homopolymers.

Considering the above all, in this study, we synthesized the monomer of 1,4-bis(2-(3,4-ethylenedioxy)thienyl)benzene (EBE) via coupling reaction under the introduction of the literature [10]. Then we successfully synthesized the copolymer by electrochemical oxidized the mixture of BMTB and EBE. The resultant copolymer P(EBE-co-BMTB) is an multichromic materials with fine tunability of its band gaps by controlling the feed ratio of two monomers. The opto-electrochemical and electrochromic properties of the copolymer were also investigated. Additionally, we constructed dual type electrochromic devices (ECDs) where the P(EBE-co-BMTB) copolymer and PEDOT functioned as the anodically and cathodically coloring material, respectively. Characterizations of the electrochromic behavior of the ECDs were achieved by spectroelectrochemistry, kinetic and stabilities study.

2. EXPERIMENTAL

2.1. Materials

1,4-Dibromobenzene, 3,4-ethylenedioxythiophene (EDOT, 98%), tri-n-butyltin chloride (SnBu_3Cl) and bis(triphenylphosphaneare) dichloropalladium ($\text{Pd}(\text{PPh}_3)_2\text{Cl}_2$) are purchased from Aldrich Chemical and used as received. Commercial high-performance liquid chromatography grade acetonitrile (ACN, Tedia Company, INC., USA), dichloromethane (DCM, Sinopharm Chemical Reagent CO., Ltd., China), poly(methyl methacrylate) (PMMA), propylene carbonate (PC), n-butyllithium (n-BuLi) and lithium perchlorate (LiClO_4 , 99.9%) are purchased from Shanghai Chemical Reagent Company and used directly without further purification. Tetrahydrofuran (THF, J&K Chemical Co. Beijing China) is distilled over Na/benzophenone prior to been used, sodium perchlorate (NaClO_4 , Shanghai Chemical Reagent Company, 98%) is dried in vacuum at 60 °C for 24 h before use. Other reagents are all used as received without further treatment. Indium-tin-oxide-coated (ITO) glass (sheet resistance: $< 10 \Omega \square^{-1}$, purchased from Shenzhen CSG Display Technologies, China) is successively washed with ethanol, acetone and deionized water under ultrasonic, and then dried by N_2 flow.

2.2. Instrumentation

FT-IR spectra is recorded on a Nicolet 5700 FT-IR spectrometer (Thermo Nicolet Co., Wisconsin, USA), where the samples are dispersed in KBr pellets. Scanning electron microscopy (SEM) measurements are taken using JEOL JSM-6380LV SEM (JEOL Ltd., Tokyo, Japan). A UV-vis spectrum is performed on a Perkin-Elmer Lambda 900 UV-vis spectrophotometer (PerkinElmer Inc., Massachusetts, USA). Digital photographs of the polymer films and device are taken by a Canon Power Shot A3000 IS digital camera.

2.3. Electrochemistry

Electrochemical syntheses and experiments are performed in a one-compartment cell with a CHI 760 C Electrochemical Analyzer (Shanghai Chenhua Instrument Co., China) under control of a computer, employing a platinum wire with a diameter of 0.5 mm as the working electrode, a platinum ring as the counter electrode, and taking a silver wire (Ag wire) as pseudo reference electrode. The solution used is ACN/DCM (1:1, by volume) containing 0.2 M NaClO_4 . The pseudo reference electrode is calibrated externally using a 5 mM solution of ferrocene (Fc/Fc^+) in the electrolyte ($E_{1/2}(\text{Fc}/\text{Fc}^+) = 0.25 \text{ V vs. Ag wire in ACN/DCM (1:1, by volume) containing 0.2 M NaClO}_4$). The half-wave potential ($E_{1/2}$) of Fc/Fc^+ measured is 0.28 V vs. SCE. Thus, the potential of Ag wire is assumed to be 0.03 V vs. SCE [21]. All of the electrochemistry experiments were performed at room temperature under nitrogen atmosphere.

2.4. Preparation for measurements

All electrochemical polymerization and CV tests are taken in ACN/DCM (1:1, by volume) containing 0.2 M NaClO₄ as a supporting electrolyte. The amount of polymers deposited on platinum electrode is controlled by the integrated charge passed through the cell for electrochemical tests. To obtain sufficient amount of polymers for spectra analysis and SEM measurements, ITO glass with a surface area of 0.9 cm × 2.0 cm is employed as the working electrode. After polymerization, electrochemical dedoping process is carried out in ACN/DCM (1:1, by volume) containing 0.2 M NaClO₄ for 15 minutes, then washed with ACN/DCM (1:1, by volume) for 3 times to remove the supporting electrolyte and oligomers/monomers. For FT-IR spectral analysis, these polymers are further dried in vacuum at 60 °C for 24 h.

2.5. Preparation of the gel electrolyte

A gel electrolyte based on poly(methyl methacrylate) (PMMA) (MW: 350,000) and LiClO₄ is plasticized with propylene carbonate (PC) to form a highly transparent and conductive gel, ACN is also included as a low-boiling point solvent to allow easy mixing of the gel components. The composition of the casting solution by weight ratio of ACN:PC:PMMA:LiClO₄ is 70:20:7:3. The gel electrolyte is used for construction of the polymer electrochromic device [22].

2.6. Fabrication of electrochromic devices (ECDs)

ECDs are constructed using two polymers, namely P(EBE-co-BMTB) as the anodically material and PEDOT as the cathodically material. The P(EBE-co-BMTB) and PEDOT films are electrodeposited onto two ITO glass electrodes (active area: 1.8 cm × 2.4 cm) at +1.3 and +1.4 V, respectively. ECDs were fabricated by arranging the two polymer films (one oxidized, the other reduced) facing each other separated by the gel electrolyte.

3. RESULTS AND DISCUSSION

3.1. Electrochemical polymerization and characterization of P(EBE-co-BMTB)

3.1.1. Electrochemical polymerization

The successive CV curves of 0.004 M EBE, 0.004 M BMTB and the EBE/BMTB mixture (0.002 M EBE and 0.002 M BMTB) in ACN/DCM (1:1, by volume) containing 0.2 M NaClO₄ are illustrated in Fig. 1. As shown in Fig. 1a, the polymerization of EBE presents the anodic peak at around +0.90 V and a well-defined cathodic peak at +0.53 V. The CV curves of BMTB show two successive oxidation peaks at +1.0 V and +1.20 V and a broad reduction peak locates at +0.83 V (Fig. 1c).

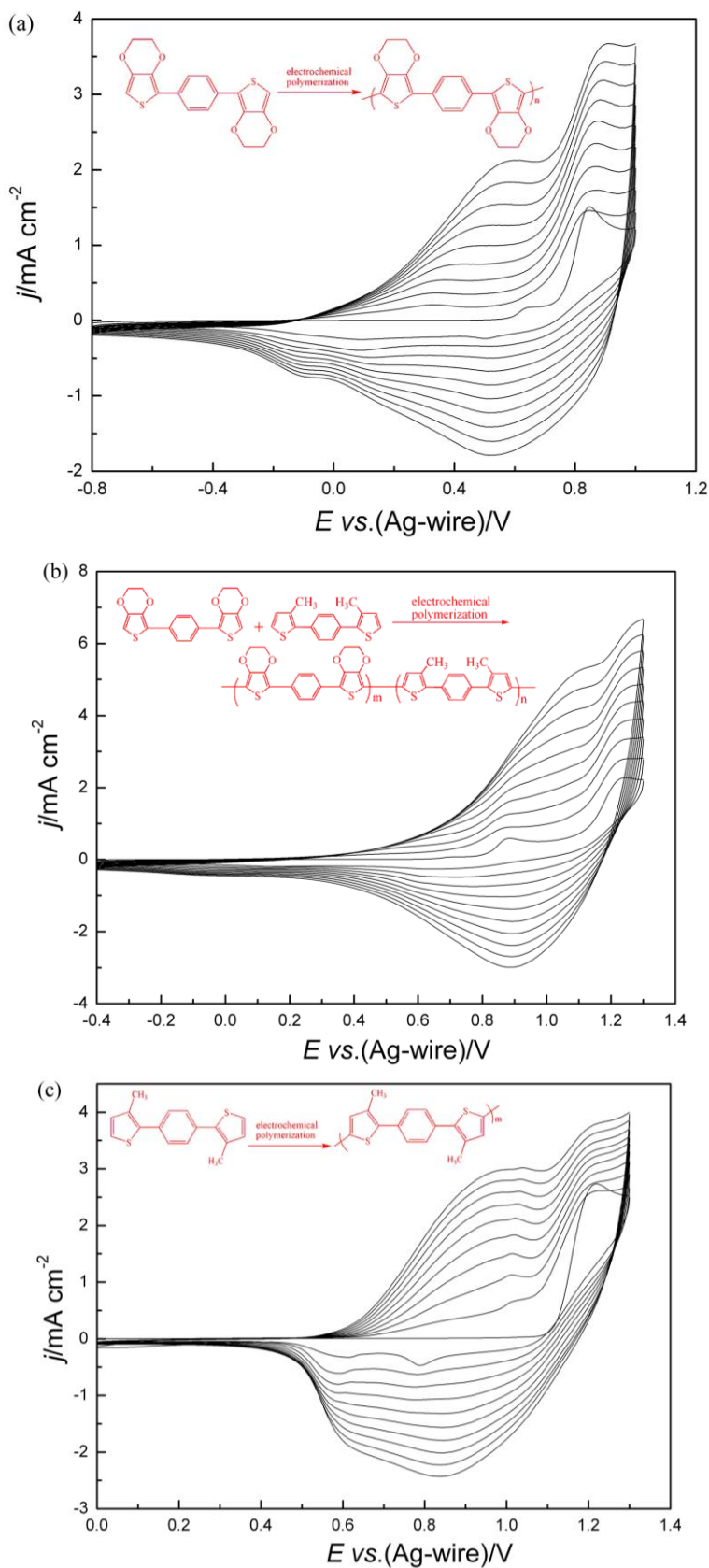


Figure 1. Successive CV curves of (a) 0.004 M EBE, (b) 0.002 M EBE and 0.002 M BMTB, (c) 0.004 M BMTB in ACN/DCM (1:1, by volume) containing 0.2 M NaClO_4 . Scanning rates: 100 mV s^{-1} . j denotes the current density, E denotes the potential.

However, the CV curves of the EBE/BMTB mixture exhibits an anodic peak at around +1.25 V and a cathodic peak at +0.90 V (Fig. 1b), which is different from those of EBE and BMTB. Besides, at the first cycle of Fig. 1b, it shows two oxidation peaks at around +0.88V and +1.25V, which can be attributed to the oxidation of EBE and BMTB monomers, respectively, which indicating the formation of a new copolymer (P(EBE-co-BMTB)) consisting of both EBE and BMTB units [28–30]. Furthermore, as can be seen from Fig. 1, there is an obvious increase of current density of the EBE/BMTB mixture compared with those of EBE and BMTB, which can also imply the formation of a copolymer [29].

3.1.2. Electrochemistry behavior of P(EBE-co-BMTB) films

Fig. 2 shows the electrochemical behavior of the P(EBE-co-BMTB) film (prepared on platinum wires by sweeping the potentials from -0.4 and $+1.3$ V for three cycles) at different scan rates between 25 and 300 mV s^{-1} in ACN/DCM (1:1, by volume) containing 0.2 M NaClO_4 . As can be seen from Fig. 2, the copolymer film is cycled repeatedly between doped and dedoped states without significant decomposition and exhibits a reversible redox process between $+0.78$ and $+1.15$ V. Scan rate dependence experiments showed that both anodic and cathodic peak currents increase linearly with increasing scan rate (see insert of Fig. 2), which indicating a well adhered copolymer film on the working electrode surface [31]. This also demonstrates that the electrochemical processes of P(EBE-co-BMTB) are reversible and not diffusion limited [15,26].

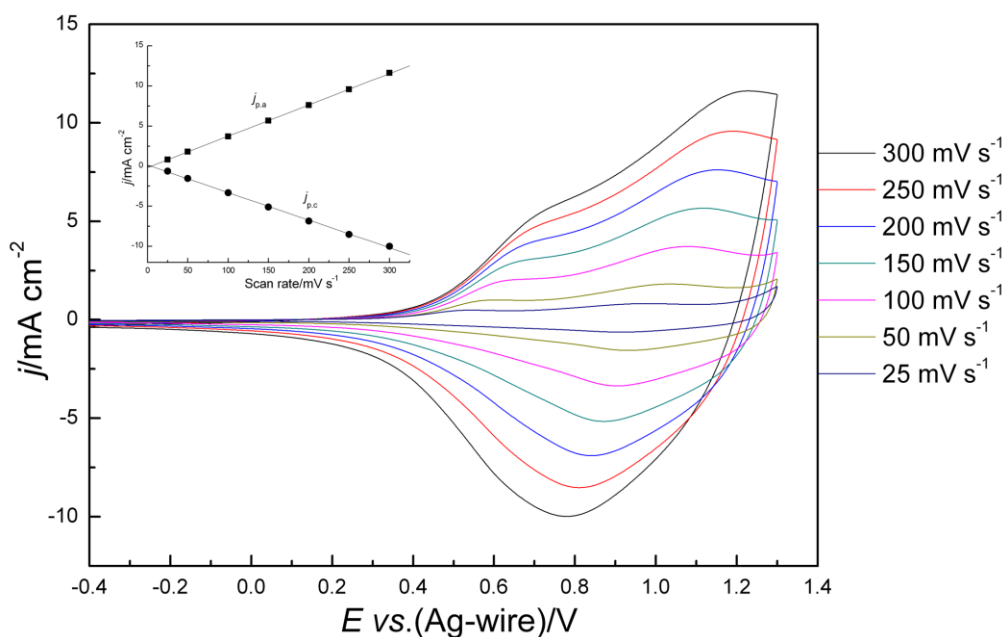


Figure 2. CV curves of the P(EBE-co-BMTB) film at different scan rates between 25 and 300 mV s^{-1} in the monomer-free ACN/DCM (1:1, by volume) containing 0.2 M NaClO_4 , j denotes the current density, E denotes the potential. Insert: Scan rate dependence of the P(EBE-co-BMTB), j_{pa} and j_{pc} denote the anodic and cathodic peak current densities, respectively.

3.1.3. FT-IR spectra of PEBE, P(EBE-co-BMTB) and PBMTB

The FT-IR spectra of PEBE, P(EBE-co-BMTB) and PBMTB obtained under different applied potentials are shown in Fig. 3. According to the spectrum of PBMTB (Fig.3a), the absorption peak at 829 cm^{-1} is due to the C–H out-of-plane bending vibrations of a 2,3,5-trisubstituted thiophene ring [18], the peaks located at 1377 and 1450 cm^{-1} are assigned to the deformation of the methyl ($-\text{CH}_3$) group [32]. In the spectrum of PEBE (Fig. 3c), the bands at 1189 and 1075 cm^{-1} are assigned to the stretching of the C–O–C bond in EDOT ring [33]. The above mentioned bands of PBMTB and PEBE could also be found in the FT-IR spectrum of P(EBE-co-BMTB) (Fig. 3b). Compared with corresponding homopolymers, the band at 827 cm^{-1} in the spectrum of P(EBE-co-BMTB) originates from the out-of-plane of C–H bending vibrations of 2,3,5-trisubstituted thiophene ring, indicating the presence of BMTB units in the copolymer. While the bands at 1189 and 1078 cm^{-1} in the copolymer can also be ascribed to the stretching of the C–O–C bond in EBE monomer. All the above features indicate that the copolymer P(EBE-co-BMTB) contain both BMTB and EBE units.

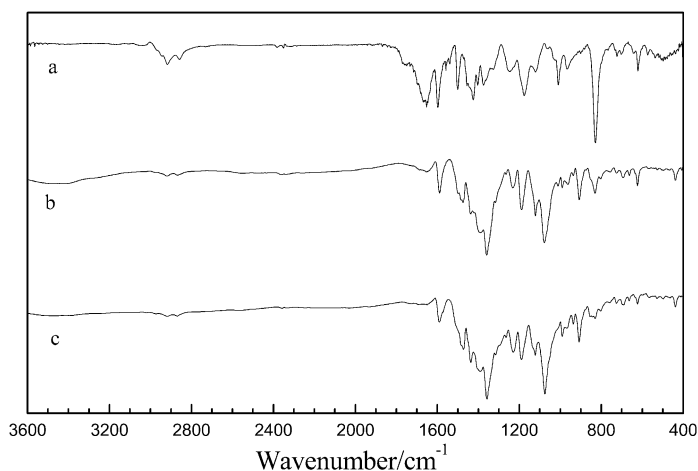


Figure 3. The FT-IR spectra of (a) PBMTB, (b) P(EBE-co-BMTB) and (c) PEBE obtained at +1.3 V, +1.3 V and +1.0 V potentiostatically in ACN/DCM (1:1, by volume) solution containing 0.2 M NaClO_4 , respectively.

3.1.4. Scanning electron microscopy

Scanning electron micrographs (SEM) of polymers provide their clear surface and bulk morphologies, PEBE, P(EBE-co-BMTB) and PBMTB were deposited on ITO glass electrode ($0.5\text{ cm} \times 0.5\text{ cm}$) at +1.0 V, +1.3 V and +1.3 V potentiostatically in ACN/DCM (1:1, by volume) solution containing 0.2 M NaClO_4 , respectively, and then dedoped for 300 s. The SEMs of them are shown in Fig. 4. In this case, The PEBE film exhibits a compact accumulation state of clusters of granules (Fig. 4a). PBMTB exhibits porous structure with a great deal of globules, and the approximate diameters of these globules are in the range of 100–1000 nm (Fig. 4c). While P(EBE-co-BMTB) shows an irregular porous structure with huge amounts of tiny granules stacked together (Fig. 4b), which are different

from two corresponding homopolymers. The difference of morphology between P(EBE-co-BMTB) and the homopolymers also confirms the occurrence of copolymerization between EBE and BMTB.

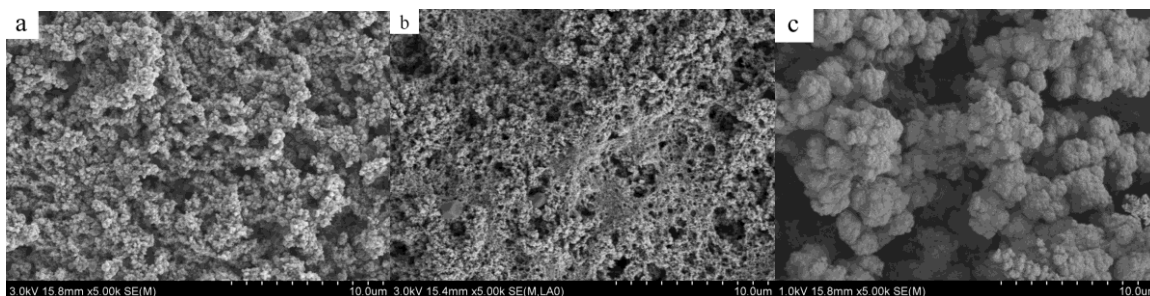


Figure 4. SEM images of (a) PEBE, (b) P(EBE-co-BMTB) and (c) PBMTB deposited potentiostatically on ITO electrode.

3.1.5. UV-vis spectra of PEBE, PBMTB and P(EBE-co-BMTB)

Fig. 5 depicts the UV-vis spectra of dedoped (a) PBMTB, (b) P(EBE-co-BMTB) and (c) PEBE deposited on ITO electrode with the same polymerization charge (3.2×10^{-2} C) at +1.3 V, +1.3 V and +1.0 V, respectively. In the neutral state, PBMTB film exhibits an absorption band at 411 nm due to the $\pi-\pi^*$ transition (Fig. 5a). As shown in Fig. 5c, the neutral state PEBE exhibits the $\pi-\pi^*$ electron transition peak at about 511 nm. However, it should be noted that the maximum absorption band of the neutral state P(EBE-co-BMTB) copolymer was centered at 456 nm (Fig. 5b), which are attributed to the $\pi-\pi^*$ transition. Compared with the maximum absorption peak of PBMTB film, there is an obvious red shift due to the introduction of EBE units into copolymer main chain, which further confirms the occurrence of the copolymerization of BMTB with EBE.

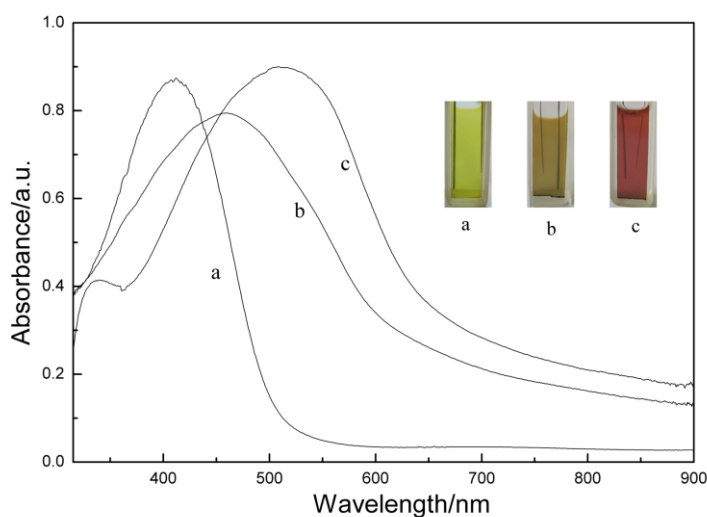


Figure 5. UV-vis spectra of (a) PBMTB, (b) P(EBE-co-BMTB) and (c) PEBE deposited on ITO glass. Insert: the neutral state color images of (a) PBMTB, (b) P(EBE-co-BMTB) and (c) PEBE films on ITO glass.

Table 1 summarized the onset oxidation potential (E_{onset}), maximum absorption wavelength (λ_{max}), low energy absorption edges (λ_{onset}), HOMO and LUMO energy levels and the optical band gaps (E_g) values ($E_g = 1241/\lambda_{\text{onset}}$) of PBMTB, PEBE and the copolymers (prepared with the feed ratio of EBE/BMTB at 2:1 (COP1), 1:1 (COP2) and 1:2 (COP3), respectively) quite clearly. HOMO energy levels of them were calculated by using the formula $E_{\text{HOMO}} = -e(E_{\text{onset}} + 4.4)$ (vs. SCE) and LUMO energy levels (E_{LUMO}) of them were calculated by the subtraction of the optical band gap (E_g) from the HOMO levels [34]. We concluded from the data of Table 1 that we could introduce EBE units into PBMTB chains to tuning the band gap of PBMTB film, thus we can obtain target copolymers with intent band gap value, through control of the feed ration of EBE monomer.

Table 1. The onset oxidation potential (E_{onset}), maximum absorption wavelength (λ_{max}), onset absorption wavelength (λ_{onset}), HOMO and LUMO energy levels and optical band gap (E_g) of PEBE, PBMTB and COP1, COP2, COP3 (prepared with the feed ratio of EBE/BMTB at 2:1, 1:1 and 1:2, respectively).

Compounds	E_{onset} , vs.(Ag-wire) (V)	λ_{max} (nm)/ λ_{onset} (nm)	E_g^a (eV)	HOMO (eV)	LUMO ^b (eV)
PEBE	0.772	510/638	1.945	-5.202	-3.257
COP1	0.777	481/627	1.979	-5.207	-3.228
COP2	0.784	460/617	2.011	-5.214	-3.203
COP3	0.801	436/596	2.082	-5.231	-3.149
PBMTB	1.120	411/502	2.472	-5.550	-3.078

^a Calculated from the low energy absorption edges (λ_{onset}).

^b Calculated by the subtraction of the optical band gap (E_g) from the HOMO level.

3.2. Electrochromic properties of P(EBE-co-BMTB)

3.2.1. Spectroelectrochemical properties of P(EBE-co-BMTB)

One of the important means of studying the changes in the absorption spectra and characterizing the electronic structures of conjugated polymers is spectroelectrochemistry. P(EBE-co-BMTB) coated ITO glass (prepared potentiostatically at +1.30 V vs. Ag wire) was switched between -0.4 V and +1.20 V in ACN/DCM (1:1, by volume) containing 0.2 M NaClO₄ solution in order to obtain the UV-vis spectra (Fig. 6). In the neutral state, the copolymer film exhibits an absorption band at 432 nm due to the π - π^* transition. As shown in Fig. 6, the intensity of the P(EBE-co-BMTB) π - π^* electron transition absorption decreases while the charge carrier absorption bands located at around 730 nm increase dramatically upon oxidation. The appearance of charge carrier bands could be attributed to the evolution of polaron and bipolaron bands.

In addition, the P(EBE-co-BMTB) film shows color electrochromism under various potentials. In order to study the range of colors, a wide interval of potentials (-0.4 V to +1.3 V) was applied on the as-prepared P(EBE-co-BMTB) films. As can be seen from Fig. 6, P(EBE-co-BMTB) film showed distinctive colors in neutral and oxidized states. The orange yellow color of the film at neutral state

(−0.4 V) turned into yellowish green color (+0.5 V) and sky blue color (+0.9 V), and finally exhibited purplish blue color at full doped state (+1.30 V). This multicolor property possesses significant potential applications in smart windows or displays.

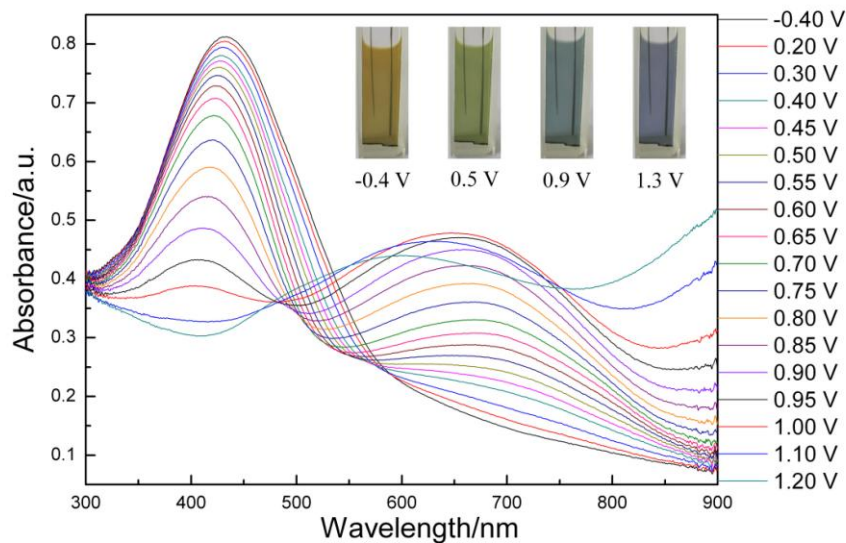


Figure 6. Spectroelectrochemical spectra of P(EBE-co-BMTB) with applied potentials between −0.4 V and +1.2 V in monomer-free ACN/DCM (1:1, by volume) containing 0.2 M NaClO₄ solution.

3.2.2. Electrochromic switching of P(EBE-co-BMTB) film

It is important that electrochromic polymers can switch rapidly and exhibit a noteworthy color change for electrochromic applications [35]. For this purpose, double potential step chronoamperometry technique was used to investigate the switching ability of P(EBE-co-BMTB) film between its neutral and full doped states. The dynamic electrochromic experiment for P(EBE-co-BMTB) was performed at 675 nm and 430 nm, respectively. The potential was switched between −0.4 V (the neutral state) and +1.3 V (the oxidized state) with regular intervals of 4 s. Another important characteristic of electrochromic materials is the optical contrast ($\Delta T\%$), which can be defined as the transmittance difference between the redox states. The maximum $\Delta T\%$ of the P(EBE-co-BMTB) was calculated to be 31.1% at 430 nm and 19.3% at 630 nm, as showed in Fig. 7.

The coloration efficiency (CE) is also an important characteristic for the electrochromic materials. CE can be calculated by using the equations given below [36,37]:

$$\Delta OD = \log \left(\frac{T_b}{T_c} \right) \text{ and } \eta = \frac{\Delta OD}{\Delta Q}$$

where T_b and T_c are the transmittances before and after coloration, respectively. ΔOD is the change of the optical density, which is proportional to the amount of created color centers. η denotes the coloration efficiency (CE). ΔQ is the amount of injected charge per unit sample area. CE of

P(EBE-co-BMTB) film was measured as $126.2 \text{ cm}^2 \text{ C}^{-1}$ (430 nm) and $79.7 \text{ cm}^2 \text{ C}^{-1}$ (675 nm), respectively, which had reasonable coloration efficiency.

Response time, one of the most important characteristics of electrochromic materials, is the necessary time for 95% of the full optical switch (after which the naked eye could not sense the color change) [35,38]. The response time was found to be 2.3 s from the reduced to the oxidized state and 0.41 s from the oxidized to the reduced state at 430 nm, 0.83 s from the reduced to the oxidized state and 1.54 s from the oxidized to the reduced state at 675 nm. Compare with the electrochromic switching of PBMTB film reported earlier [19], the P(EBE-co-BMTB) film has lower optical contrast and higher coloration efficiency, which is due to the introduction of EBE units in the polymer backbone.

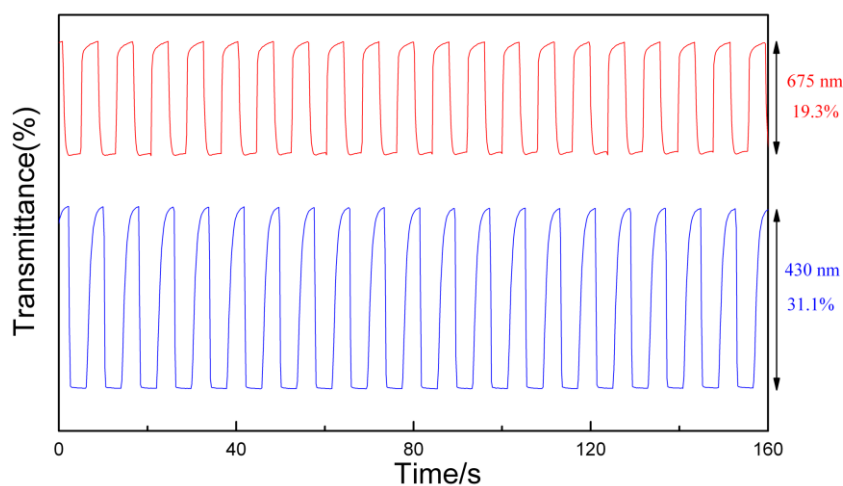


Figure 7. Electrochromic switching for P(EBE-co-BMTB) film under an applied square voltage signal between -0.4 V and $+1.30 \text{ V}$ with a residence time of 4 s at 430 nm and 675 nm, respectively.

3.3. Spectroelectrochemistry of electrochromic devices (ECDs)

3.3.1. Spectroelectrochemical properties of ECD

A dual type ECD consisting of P(EBE-co-BMTB) and PEDOT was constructed and its spectroelectrochemical behavior was also studied. Before composing the ECD, the cathodically coloring polymer (PEDOT) was fully oxidized while the anodically coloring polymer film (P(EBE-co-BMTB)) was fully reduced. The spectroelectrochemical spectra of the P(EBE-co-BMTB)/PEDOT device as a function of applied potential (between -0.8 V and 1.4 V) was given in Fig.8. The spectroelectrochemical result shows P(EBE-co-BMTB) layer is in its neutral state, where the absorption at 438 nm was due to $\pi-\pi^*$ transition of the copolymer. At that state, device revealed grayish green color due to electrochromic device was constructed based on orange yellow P(EBE-co-BMTB) and light blue PEDOT on the basis of color mixing theory. As the applied potential increased, the P(EBE-co-BMTB) layer start to be oxidized while PEDOT layer was reduced, the peak at 438 nm

was decreased, while the absorption band at 625 nm was increased (Fig. 8), and the dominated color of the device is sky blue at +1.4 V.

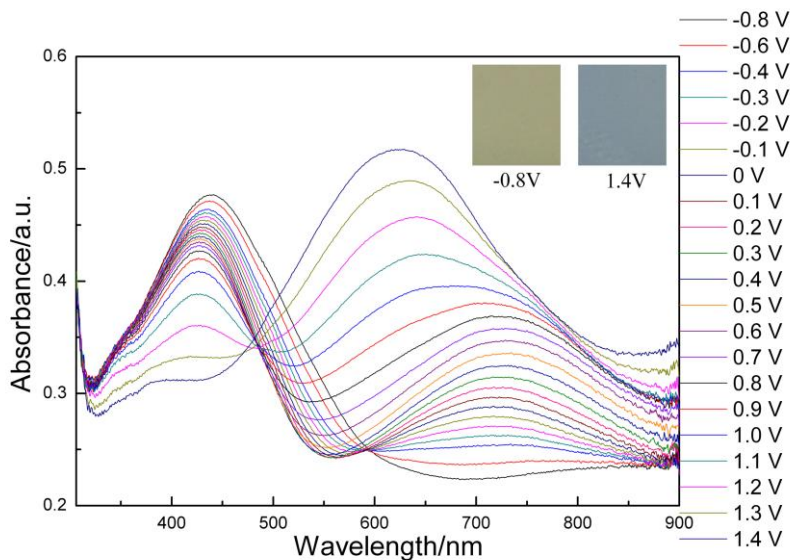


Figure 8. Spectroelectrochemical spectra P(EBE-co-BMTB)/PEDOT device at various applied potentials from -0.8 to $+1.4$ V.

3.3.2. Switching of ECD

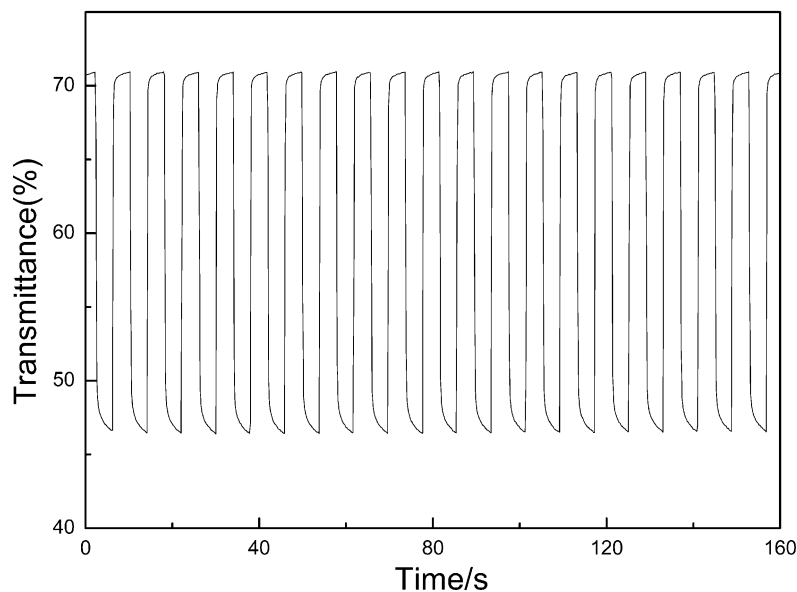


Figure 9. Electrochromic switching, optical response for P(EBE-co-BMTB)/PEDOT device by applying potentials between -0.8 V (the neutral state) and $+1.4$ V (the oxidized state) with a residence time of 4 s.

Kinetic studies were also done to test the response time of P(EBE-co-BMTB)/PEDOT ECD. Under a square potential input of -0.8 and $+1.4$ V at regular intervals of 4 s, the optical response at 630 nm, as illustrated in Fig. 9, was found to be 1.05 s at 95% of the maximum transmittance from the neutral state to oxidized state and 0.22 s from the oxidized state to the neutral state, and $\Delta T\%$ was calculated to be 24.5 %. The CE of the device (the active of area is $1.8 \text{ cm} \times 1.8 \text{ cm}$) was calculated to be $397.9 \text{ cm}^2 \text{ C}^{-1}$ at 630 nm. The spectroelectrochemical spectra and the optical response of PBMTB/PEDOT device have been also reported by our group [19]. Contrary to the our expectation, the P(EBE-co-BMTB)/PEDOT device did not present high optical contrast (24.5%) and fast response time (0.22 s) compared with the PBMTB/PEDOT device. Even if it is usually improve the properties of the switching of ECD, when introduce 3,4-ethylenedioxythiophene units into the anodically coloring polymer film. However, the reasonable optical contrast and satisfactory response time indicating the P(EBE-co-BMTB)/PEDOT ECD has potential applications.

3.3.3. Open circuit memory of ECD

The optical memory in the electrochromic devices is another important parameter since it is directly related to its application and energy consumption during the use of ECDs [38,39]. The optical spectra for P(EBE-co-BMTB) was monitored at 630 nm as a function of time at -0.8 and $+1.4$ V by applying the potential for 1 s for 100 s time intervals. As seen in Fig. 10, at grayish green colored state device shows a true permanent memory effect since there is almost no transmittance change under applied potential or open circuit conditions. In sky blue colored state device is rather less stable in terms of color persistent, however this matter can be overcome by application of current pulses to freshen the fully colored states.

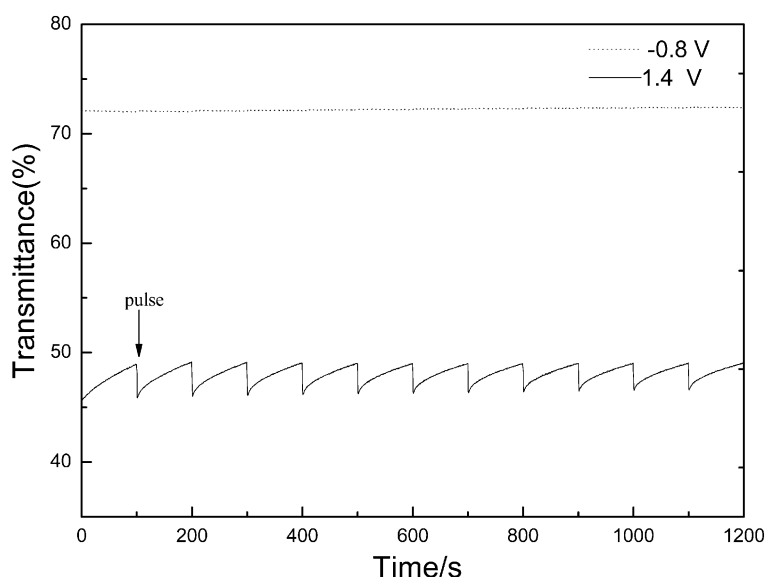


Figure 10. Open circuit stability of the P(EBE-co-BMTB)/PEDOT ECD monitored at 630 nm.

3.3.4. Stability of ECD

The stability of the devices toward multiple redox switching usually limits the utility of electrochromic materials in ECD applications. Therefore, redox stability is another important parameter for ECD [40,41]. For this reason, the P(EBE-co-BMTB)/PEDOT ECD was tested by cycling of the applied potential between -0.8 and $+1.4$ V with 500mV/s to evaluate the stability of the devices (Fig. 11). After 1000 cycles, 85.4% of its electroactivity is retained and the changes in anodic (j_{pa}) and cathodic peak current densities (j_{pc}) were 12.6% and 17.4%, respectively. These results indicated that this ECD has reasonable redox stability.

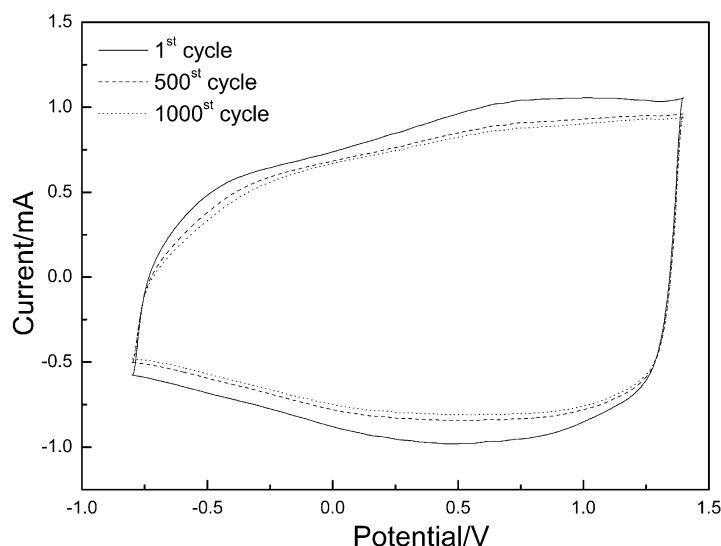


Figure 11. Cyclic voltammogram of P(EBE-co-BMTB)/PEDOT device as a function of repeated scans 500 mV/s .

4. CONCLUSIONS

A novel electrochromic copolymer based on EBE and BMTB was successfully synthesized by electrochemical oxidation of their monomers mixture. The introduction of EBE units into PBMTB chains modified the band gap of the polymer. Furthermore, according to the spectroelectrochemical analyses, the copolymer film reveals distinct electrochromic properties from those of the homopolymer film and shown four different colors (orange yellow, yellowish green, sky blue and purplish blue) under various potentials. Then, dual type ECD based on P(EBE-co-BMTB) and PEDOT was also constructed and characterized. The ECD shows grayish green color at neutral state and sky blue color at oxide state. Compared with the PBTB/PEDOT device, the P(EBE-co-BMTB)/PEDOT device did not present higher optical contrast and shorter response time. Even so, those multielectrochromic properties still make P(EBE-co-BMTB) a good candidate for potential commercial applications.

ACKNOWLEDGEMENTS

The work was financially support by the open foundation of the State key Laboratory of Electronic Thin Films and Integrated Devices (KFJJ201114).

References

1. G. Sonmez, *Chem. Commun.*, 42 (2005) 5251.
2. I.Osken, H. Bildirir, T. Ozturk, *Thin Solid Films.*, 519 (2011)7707.
3. J. H.Burroughes, D. D. C. Bradley, A. R.Brown, R. N. Marks, K. Mackay, R.H. Friend, P.L. Burns, A. B.Holmes, *Nature* 347 (1990)539.
4. B. B.Carbas, A.Kivrak, A. M.Önal, *Electrochim. Acta* 58(2011) 223.
5. H.Ma, H.L.Yip, F.Huang, A. K.Y Jen, *Adv. Funct. Mater.* 20(2010) 1371.
6. M. Ak, M.S.Ak, G. Kurtay, M. Güllü, L. Toppare, *Solid State Sci.* 12 (2010) 1199.
7. F. B. Koyuncu, S.Koyuncu, E. Ozdemir, *Org. Electron.* 12 (2011) 1701.
8. S.Varis, M. AK, C. Tanyeli, I. M.Akhmedov, L.Toppare, *Eur. Polym. J.*, 42 (2006) 2352.
9. C. Zhang, C. Hua, G.H. Wang, M.Ouyang, C.A. Ma, *Electrochim. Acta.*, 55 (2010) 4103
10. A.M. Fraind, J. D.Tovar, *J. Phys. Chem. B* 114 (2010) 3104.
11. O.Turkarlan, M. Ak, C. Tanyeli, I. M. Akhmedov, L.Toppare, *J. Polym. Sci: Part A: Polym. Chem.* 45(2007) 4496.
12. P. R.Somani, S. Radhakrishnan, *Mater. Chem. Phys.*, 77(2002) 117.
13. C. Pozo-Gonzalo, M.Salsamendi, J.A.Pomposo, H. J. Grande, E.Y.Schmidt, Y.Rusakov, B.A. Trofimov, *Macromolecules* 41(2008) 6886.
14. Y. H. Pang, X.Y.Li, H. I.Ding, G.Y.Shi, L.T.Jin, *Electrochim. Acta* 52(2007) 6172.
15. D.Asil, A.Cihaner, F.Algi, A. M.Önal, *J. Electroanal. Chem.*, 618(2008) 87.
16. B.Wang, J. S.Zhao, R. M.Liu, J. F.Liu, Q.P.He, *Sol. Energy Mater. Sol. Cells.*, 95(2011) 1867.
17. M. J. Yang, Q. H.Zhang, P.Wu, H.Ye, X.Liu, *Polymer.*, 46(2005) 6266.
18. S. Q.Xiao, H. X.Zhou, W.You, *Macromolecules.*, 41(2008) 5688.
19. B.Wang, J.S.Zhao, C.S.Cui, J. F. Liu, Q. P. He, *Sol. Energy Mater. Sol. Cells.*, 98(2012) 161.
20. G. A.Sotzing, J. R.Reynolds, P.J.Steel, *Chem. Mater.*, 8(1996) 882.
21. G.Sonmez, C. K. F.Shen, Y.Rubin, F.Wudl, *Angew. Chem. Int. Ed.*, 116 (2004) 1524.
22. Sonmez, G., Meng, H., & Wudl, F. *Chem. Mater.* 16, 5574–580 (2004).
23. X. B.Wan, W.Zhang, S.Jin, G.Xue, Q. D You, B. Che, *J. Electroanal. Chem.* 470(1999) 23
24. G. M.Nie, L.Y.Qu, Y.Zhang, J. K Xu, S.S. Zhang, *J. Appl. Polym. Sci.* 109(2008) 373.
25. S.Kuwabata, S. Ito, H.Yoneyama, *J. Electrochem. Soc.* 135(1988)1691
26. C. Zhang, Y. Xu, N.C. Wang, Y.Xu, W.Q.Xiang, M. Ouyang, C.A. Ma, *Electrochim. Acta* 55(2009) 13.
27. V.Seshadri, L.Wu, G. A. Sotzing, *Langmuir* 19(2003) 9479.
28. C.Kvarnström, H.Kulovaara, P. Damlin, T.Vuorinen, H.Lemmetyinen, A.Ivaska, *Synth. Met.* 149 (2005) 39.
29. G.M.Nie, L.Y.Qu, J.K. Xu, S.S. Zhang, *Electrochim. Acta* 53 (2008) 8351.
30. S. Demoustier-Champagne, J.R.Reynolds, M. Pomerantz, *Chem. Mater.*, 7(1995) 277.
31. G. W.Lu, G.Q.Shi, *J. Electroanal. Chem.*, 586(2006) 154.
32. P.Camurlu, C.Gultekin, Z.Bicil, *Electrochim. Acta* 61(2012) 50.
33. Z.H.Weil, J. K.Xu, J.Hou, W.Q. Zhou, S. Z.Pu, *J. Mater. Sci.* 41(2006) 3923.
34. L.T.Huang, H.J.Yen, J.H.Wu, G.S Liou, *Org. Electron.*,13(2012) 840.
35. G. M Nie, L. J. Zhou, Q. F.Guo, S.S. Zhang, *Electrochem. Commun.* 12(2010) 160.
36. C.Bechinger, M. S.Burdis, J.G.Zhang, *Solid State Commun.* 101(1997)753.
37. W.Yang, J. S.Zhao, Y.Kong, T.Y.Kong, C.S. Cui, *Int. J. Electrochem. Sci.* 7 (2012) 2764.
38. B.Yigitsoy, S.Varis, C.Tanyeli, I. M.Akhmedov, L.Toppare, *Electrochim. Acta* 52(2007) 6561

39. Yang, W., Zhao, J. S., Cui, C. S., Kong, Y., Zhang, X.X., and Li, P. *J. Solid State Electrochem.*
doi:10.1007/s10008-012-1820-6 (in the press).
40. W.A.Gazotti Jr, G. Casalbore-Miceli, A.Geri, M.A. D. Paoli, *Adv. Mater.* 10(1998) 60.
41. R. J.Mortimer, T. S. Varley, *Chem. Mater.* 23(2011) 4077.

© 2012 by ESG (www.electrochemsci.org)